

Reduction of unsteadiness in the transonic flow past an axisymmetric afterbody with two boosters

P. Meliga and P. Rejjasse**

**ONERA, Département d'Aérodynamique Fondamentale et Expérimentale
8 rue des Vertugadins, 92190 Meudon, France*

Abstract

The transonic flow past a three-dimensional afterbody is investigated experimentally through wall-pressure measurements. We use a three-body geometry made of an axisymmetric main body, equipped with a propulsive nozzle and two removable cylindrical boosters mounted at diametrically opposed positions. The distance between the base plane and the nozzle exit section is chosen so that the separated flow reattaches on the external nozzle wall. Test performed in presence of a short cylindrical serrated skirt show a significant reduction of the fluctuation levels of approximately 30% in the whole separated area.

1. Introduction

Launcher afterbody flows are characterized by a massive separation occurring at the base region due to an abrupt change in the rear geometry. The unsteadiness of the separated flow generates strong low frequency wall-pressure fluctuations and induces aerodynamic excitation. The resulting high dynamic loads can trigger a response of the structural modes termed buffeting that can be critical during the transonic phase of flight, as experienced by the Ariane V launcher.

The properties of the base pressure of separated flows have been experimentally and theoretically studied in the last decades^{6,8,11}. For complex afterbody shapes^{1,2,4,10}, several aerodynamics phenomena are simultaneously at work (recirculating area, reattachment of the separated shear layer on a solid surface, acoustic radiation of the propulsive jet), and limit the knowledge of the dynamics. Reducing the pressure fluctuations level hence remains a challenge to improve the performances and the reliability of the future launch vehicles.

A study by Deprés et al.^{3,5} has enlightened the wall-pressure properties of axisymmetric blunt configurations equipped with a cylindrical rear-body of variable length. The main idea developed in this study is that despite the broad variety of control parameters, two main kinds of separation are to be considered, depending on whether the separated external flow does or does not reattach on the rear-body. For short rear-bodies, the flow organisation is dominated by the periodic shedding of large scale structures, as observed for bluff bodies, as shown by the far wake velocity measurements of Flodrops and Desse⁷. For sufficiently long rear-bodies, the unsteady dynamics is dominated by the reattachment process of the separated shear layer (see the review of Mabey⁹). The high intensity fluctuations can then be ascribed to the shear layer vortices impinging the downstream surface. Recent wind tunnels tests conducted on more realistic afterbody geometries made up of an axisymmetric main body equipped with two removable cylindrical boosters mounted at diametrically opposed positions¹⁰ have shown that the presence of the boosters significantly alters the dynamics, since it induces a shorter dissymmetric separated area, characterized by a massive pressure drop and high levels of fluctuations. The spatial organisation of the flow is also modified, namely the frequency and azimuthal wavenumber selection in the separation switches from the $m=1$ mode at the Strouhal number $St \sim 0.2$ corresponding to the vortex shedding phenomenon (axisymmetric afterbodies) to an $m=0$ mode at the Strouhal number $St \sim 0.35$ (three-dimensional afterbodies). This strongly contrasts with the effects reported by other authors¹. However, in this study, different afterbody shapes are involved, in particular, we believe that this difference can be ascribed to the choice of the struts device that may force the symmetry of the incoming flow.

A possible solution to reduce the flow unsteadiness is to prevent the reattachment of the shear layer. A possible technique to achieve this aim is to use skirts, whose effect is to displace downstream the separation point of the

incoming boundary layer, has been proven fruitful, although the achieved reduction remains weak compared to the fluctuations levels^{9,11}. This paper presents an experimental investigation of a three-body configuration based on wall-pressure measurements. The main goal is to assess the efficiency of a short serrated skirt to reduce the fluctuations to which the base region is submitted. We expect that the presence of teeth susceptible to promote the small-scale turbulence may significantly affect the spatial organization of the flow and enhance the effect of a classical skirt.

2. Experimental set-up

Tests are carried out in the S3Ch continuous transonic wind tunnel of ONERA. The main body is made of an axisymmetric blunt-based body of diameter $D = 100\text{mm}$ equipped with a cylindrical rear-body of diameter $d = 40\text{mm}$, whose exit plane is located at a distance $L = 120\text{mm}$ downstream of the base plane. The main body can be equipped at diametrically opposed positions with two cylindrical boosters of diameter $D_b = 65\text{mm}$ and length 576mm , whose extremity plane is located at a distance 77mm downstream of the main body base (Figure 1a). This geometry was chosen because the aspect ratio $L/D = 1.2$ allows for a reattachment of the separated shear layer on the external surface of the rear-body, in the two symmetry planes of the model¹⁰. Each booster is attached to the main body by the two struts device shown in Figure 1a, which is symmetrical with respect to the booster plane. The serrated skirt is made up of 12 teeth of length 33mm (Figure 1b). Steady and unsteady wall-pressure measurements are performed using 77 pressure taps mounted on the cylindrical forebody, the base area, and the rear-body region, both in the streamwise and azimuthal directions. Time histories of the unsteady pressures are recorded over 12 seconds. The static component is measured using 12 Statham sensors, and the fluctuating component is recorded simultaneously using 65 Kulite sensors, at a sampling rate of 10240Hz .

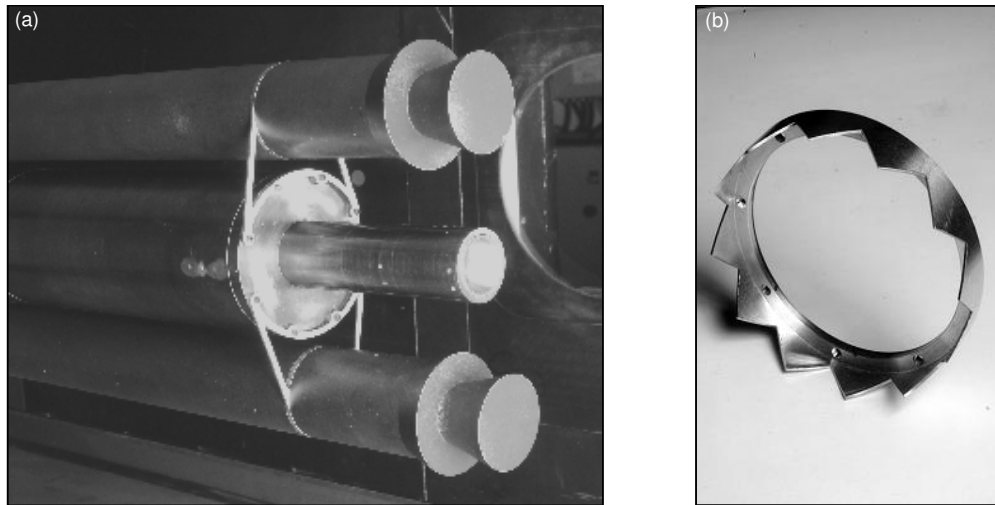


Figure 1: a) General view of the nominal configuration in the S3Ch wind tunnel. b) Detail of the serrated skirt.

The models are mounted at the end of a cylindrical forebody fixed in the wind-tunnel settling chamber, and all tests are performed at zero incidence. The no-skirt configuration, hereinafter referred to as the nominal configuration, and the skirt configuration are investigated for a free stream Mach number $M = 0.7$, the Reynolds number based on the forebody diameter D being 1.35×10^6 . The initial external boundary layer grows on the upstream cylindrical sting over a distance of over $10D$ before reaching the base corner. Both configurations are first tested without jet as a reference case. The effect of a propulsive jet at adaptation is then investigated. In this analysis, only the results with no jet are discussed here, as no significant effect of the jet was found, due to the limited interaction between the afterbody and the jet shear layers.

3. Methodology and notations

The three-body model has two symmetry planes. In the following, the B-plane denotes the booster plane, containing the axis of revolution and the boosters, and corresponding to azimuthal positions $\theta=0$ [π]. The no-booster plane, or NB-plane, is orthogonal to the B-plane and corresponds to azimuthal positions $\theta=\pi/2$ [π], as shown in Figure 2.

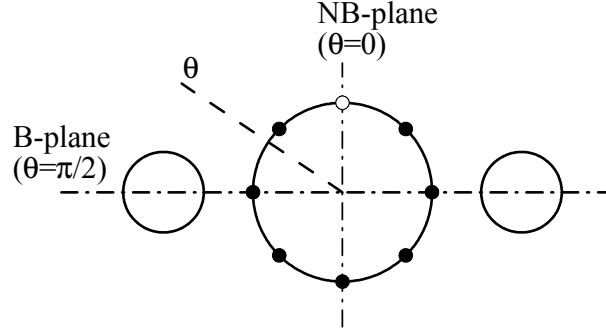


Figure 2: Geometry and location of the sensors for the correlation analysis.

We use the non-dimensional C_p and C_{prms} coefficients built on the free stream dynamic pressure q_∞ , respectively defined as

$$C_p = \frac{p - p_\infty}{q_\infty}, \quad C_{prms} = \frac{\sqrt{p'^2}}{q_\infty} \quad (1)$$

Wall-pressure spectra are investigated along the $\theta=0$ and $\theta=\pi/2$ axis, in order to estimate the three-dimensionality of the separation, and to identify the most energetic frequencies involved in the flow unsteadiness. Results are given in terms of the auto-correlation function S_{xx} and of the Strouhal number St defined as

$$St = \frac{fL}{U_\infty} \quad (2)$$

For a reference sensor located at a streamwise position x and at the azimuthal position $\theta=0$ (open symbol in Figure 2), cross-correlations are also investigated for circumferential sensor distributions located at a streamwise position $x+\Delta x$ (filled symbols in Figure 2). Considering the cross-correlation function S_{xy} between two sensors x and y , S_{xx} and S_{yy} being the respective auto-correlation functions, we investigate the normalized cross-correlation function C and its Fourier decomposition in azimuthal modes, defined as

$$C(St, \Delta\theta, \Delta x) = \frac{S_{xy}(St, \Delta\theta, \Delta x)}{\sqrt{S_{xx}(St)S_{yy}(St)}} \quad (3)$$

$$C(St, \Delta\theta, \Delta x) = \sum_m C_m(St, \Delta x) e^{im\Delta\theta} \quad (4)$$

Unless otherwise specified, Δx is set to zero, i.e. we investigate the cross-correlations in a given axial plane. Results are provided in terms of the coherence function $\gamma = |C|$ and of the azimuthal coherence function $\gamma_m = |C_m|$, which can be seen as the percentage of fluctuating energy relative to the m^{th} azimuthal mode at a given frequency.

4. Results

The streamwise distributions of C_p and $C_{p_{rms}}$ are presented in Figure 3 for both configurations. For the nominal configuration, we observe a dissymmetry of the separation with respect to the B- and NB-planes. In particular, although the recompression rates in Figure 3a are somehow similar in both planes, the recompression point is shifted downstream in the B-plane ($x/D \sim 0.55$ in the NB-plane and $x/D \sim 0.7$ in the B-plane), hence suggesting a longer separation in that plan. This is confirmed by the location of the maximum of fluctuations, indicating the reattachment of the separated shear layer, respectively at $x/D \sim 0.7$ in the NB-plane and $x/D \sim 1$ in the B-plane. The $C_{p_{rms}}$ distributions show a dramatic reduction of the pressure fluctuations, which reach $\sim 5\%$ of the upstream dynamic pressure ($\sim 9\%$ for the nominal configuration), the fluctuation levels in the NB-plane being slightly lower. Another major effect of the serrated skirt is to reduce significantly the dissymmetry of the separated area: in the NB-plane, the point of maximum fluctuations is shifted downstream, an effect that can be ascribed to the downstream displacement of the separation point of the boundary layer. However, we find no such effect in the B-plane, so that the maximum of fluctuations is located at $x/D \sim 1$ in both planes. A possible explanation is that the incoming flow is *free* in the NB-plane, i.e. the separated shear layer behaves identically to that of an axisymmetric afterbody, and *forced* in the B-plane, i.e. the reattachment length is controlled by the separation of the boundary layer developing on the boosters, as suggested by the instantaneous schlieren photograph in Figure 4. However, it remains unclear why the reduction of the pressure fluctuations is so significant in the B-plane.

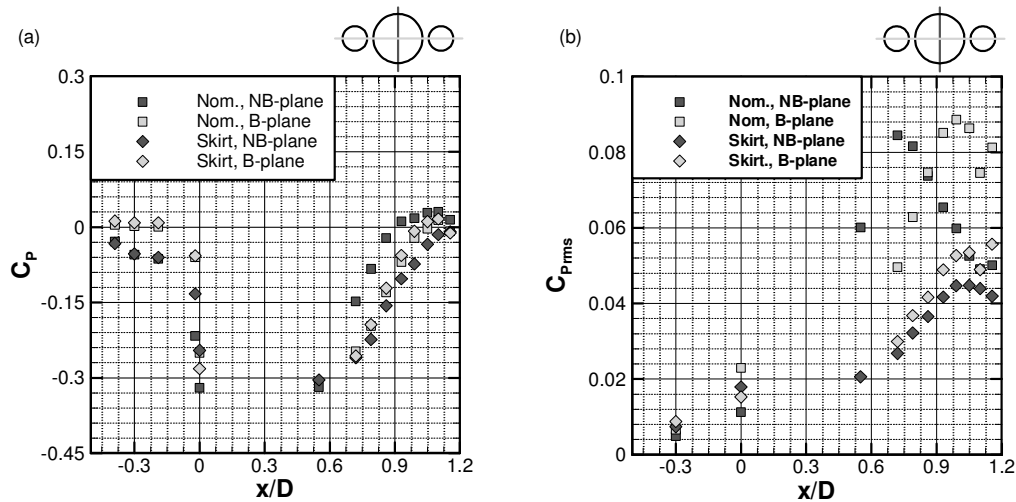


Figure 3: a) Streamwise distributions of static pressure for the nominal and skirt configurations. The dark and light symbols respectively refer to the NB- and B-planes. b) Streamwise distributions of the pressure fluctuations.

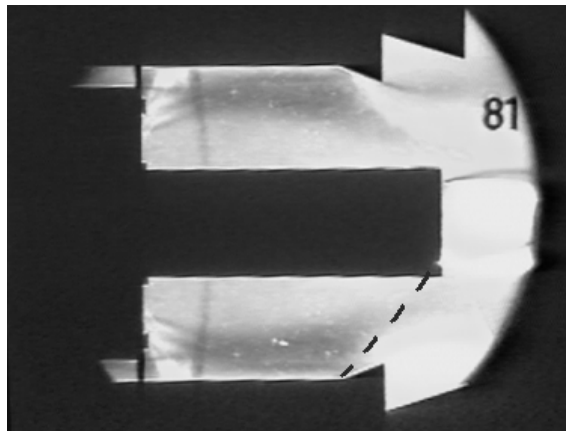


Figure 4: Schlieren photograph of the B-plane for the nominal configuration. The dashed thick line corresponds to the external envelope of the shear layer separating from the lower booster.

Figure 5 shows the power density spectra of the skirt configuration. We obtain similar pressure spectra in both planes, consistently with the idea that the skirt reduces the dissymmetry of the separated area. All spectra are dominated by a narrow peak at the Strouhal number $fL/U_\infty \sim 0.36$, whose contribution to the overall fluctuations is weak. For $x/D=1.15$, the spectra exhibit high frequency broadband fluctuations due to the shear layer vortices impinging the surface of the rear-body. The same peak is identifiable in the spectra for the nominal configuration (Figure 6), where its amplitude is significantly lower. It has been shown to be the signature of an axisymmetric mode, of azimuthal wavenumber $m=0$, that we believe to be responsible for a global coupling between the dynamics of the separated area and the dynamics of the wake developing downstream of the boosters¹⁰. The comparison between Figures 5 and 6 shows that the reduction of the pressure fluctuations in presence of the skirt are due to a lower intensity of the high frequencies. In particular, we find a dramatic reduction for $x/D=0.72$ in the NB-plane, where the shear layer reattaches without skirt, consistently with the idea that the skirt shifts the separation point downstream in that plane.

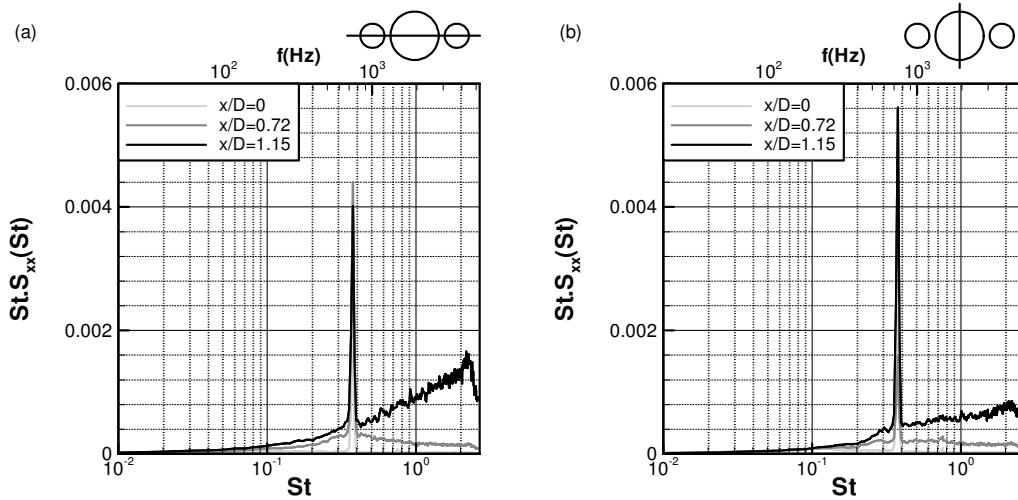


Figure 5: Spectra of the pressure fluctuations for the skirt configuration. a) B-plane. b) NB-plane.

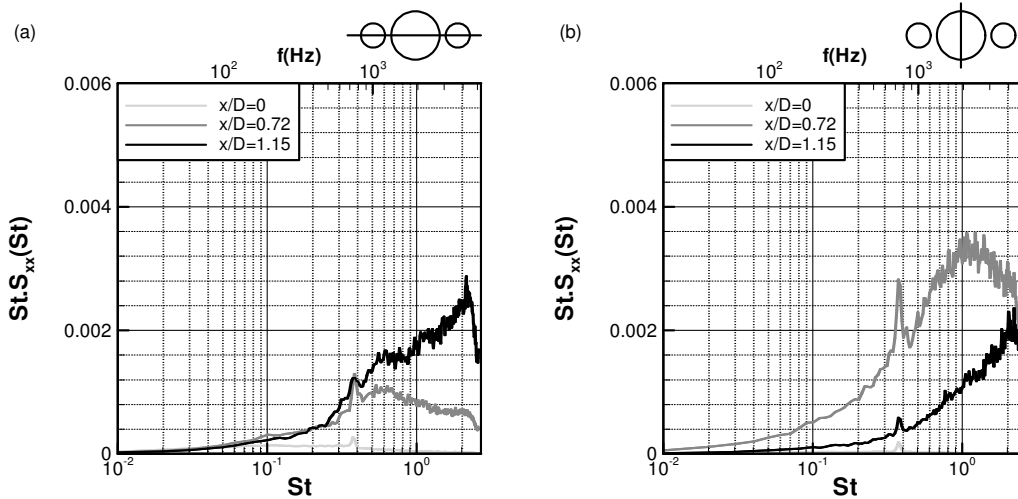


Figure 6: Spectra of the pressure fluctuations for the nominal configuration. a) B-plane. b) NB-plane.

Figure 7 presents, the coherence spectra for the skirt configuration of the modes of azimuthal wavenumbers $|m| \leq 2$ within the separation, i.e. the Fourier decomposition of the complex coherence function as a function of the frequency. We find that the $fL/U_\infty \sim 0.36$ peak is due to a highly coherent $m=0$ mode, whose energy represents 90% of the pressure fluctuations measured at this frequency. Figure 8 presents the coherence spectra of the $m=0$ mode, where the reference sensor is fixed at $x/D=1.15$, and the streamwise distance between this sensor and the circumferential distribution of sensors is varied from $\Delta x=0$ to 1.15. For the skirt configuration (Figure 8a), it

confirms that the $m=0$ mode triggers a global coupling in the whole separation, as its level of coherence remains high ($\sim 90\%$ of the pressure fluctuations) and independent of Δx . Note that this striking feature is less clear in the nominal configuration, where the level of coherence decreases as Δx increases (the level of fluctuations associated to the mode decreasing from $\sim 60\%$ to $\sim 35\%$). This azimuthal coherence analysis shows that the flow organization is identical for both configurations. In particular the presence of teeth does not seem to be significant, and similar results should be obtained by use of a short smooth skirt.

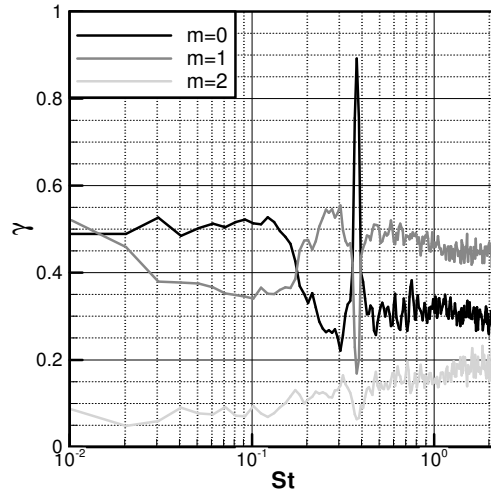


Figure 7: Coherence spectra of the first three azimuthal modes (skirt configuration).

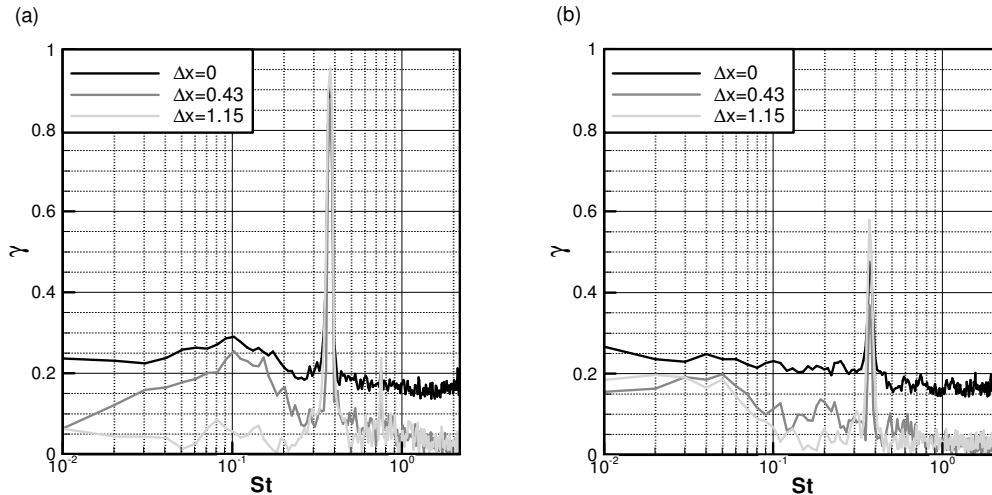


Figure 8: Coherence spectra of the $m=0$ mode for a reference sensor and a circumferential distribution of sensors located in different planes. a) Skirt configuration. b) Nominal configuration.

5. Conclusion

Wall pressure measurements have been performed on a three-body afterbody configuration in the high subsonic regime. A short cylindrical serrated skirt placed at the base of the afterbody has been tested, the main objective being to reduce buffet excitation in the separation. By displacing downstream the separation point in the NB-plane, the skirt reduces the dissymmetry of the separation seen in the nominal configuration. We also find a significant reduction of the fluctuation levels, due to lower intensities of the broadband high frequencies associated to the interaction between the shear layer vortices and the rear-body surface. However, no effect of the teeth was found, whereas the device was expected to modify the spatial organization of the separated flow region by enhancing small

scale turbulence. Further studies would be necessary to characterize the influence of the skirt shape. In particular the use of a similar skirt with an odd number of teeth may lead to very different results by breaking the symmetry of the incoming flow.

Acknowledgements

The authors thank the Centre National d'Etudes Spatiales (CNES) for financial support within the framework of the research and technology program ATAC (Aérodynamique des Tuyères et Arrière-Corps). The Ph.D. dissertation of P. Meliga is funded by CNES and ONERA.

References

- [1] David, C. and Radulovic S. Prediction on buffet loads on the Ariane 5 Afterbody. In *6th International Symposium on Launcher Technologies*, Munich, 2005.
- [2] Détery, J. and Sirieix M. Base flow behind missiles. In *AGARD LS-98 Conference*, 1979.
- [3] Deprés, D., Analyse physique et modélisation des instationnarités dans les écoulements d'arrière-corps transsoniques. PhD thesis, ONERA, 2003.
- [4] Deprés, D., Radulovic, S. and Lambaré, H. Reduction of unsteady effects in afterbody transonic flows. In *6th International Symposium on Launcher Technologies*, Munich, 2005.
- [5] Deprés, D., Reijasse P. and Dussauge J.P. Analysis of unsteadiness in afterbody transonic flows. *AIAA Journal*, 42:2541-2550, 2004.
- [6] Eldred, K.M. Base pressure fluctuations. *Journal of the Acoustical Society of America*, 33:59-63, 1961.
- [7] Flodrops, J.P. and Desse J.M. Sillage d'un Culot Axisymétrique, Inst. de Mécanique des Fluides de Lille, Rept. 85L/19, 1985.
- [8] Mabey, D.G. Some measurements of base pressure fluctuations at subsonic and supersonic speeds. Aeronautical Research Council, ARC-CP-1204, 1972.
- [9] Mabey, D.G. Pressure fluctuations caused by separated bubble flows at subsonic speeds. Royal Aircraft Establishment, Bedford, England. RAE-TR-71160, 1971.
- [10] Meliga, and P., Reijasse. Unsteady transonic flow behind an axisymmetric afterbody equipped with two boosters. In *25th AIAA Applied Aerodynamics Conference*, Miami, 2007.
- [11] Meliga, P., Reijasse P. and Chomaz J.M. Effect of a serrated skirt on the buffeting phenomenon in transonic afterbody flows. In *IUTAM Symposium on Unsteady Separated Flows and their Control*, Corfu, 2007.
- [12] Merz R.A. Subsonic base pressure fluctuations. *AIAA Journal*, 17:436-438, 1979.